

Vibration Damping Characterization of Linseed Oil-Based Elastomers for Its Effectiveness to Attenuate Structural Vibration

Rakesh Das,¹ Rajesh Kumar,² Patit P. Kundu¹

¹Department of Polymer Science and Technology, University of Calcutta, Kolkata 700009, India

²Precision Metrology Laboratory, Department of Mechanical Engineering, Sant Longowal Institute of Engineering & Technology, Sangrur, Punjab 148106, India

Correspondence to: P. P. Kundu (ppk923@yahoo.com).

ABSTRACT: Vibration damping properties of elastomers prepared from linseed oil were characterized by dynamic mechanical analyzer in a temperature range of -50 to 100°C and frequency range of 5 Hz to 1 kHz. The maximum damping loss factor, $(\tan \delta)_{\text{max}}$ varies from 0.78 to 1.32 , the room temperature (25°C) loss factor, $(\tan \delta)_{\text{rt}}$ in the range of 0.56 – 1.08 and the temperature range (ΔT) for effective damping ($\tan \delta \geq 0.3$) varies from 63°C to 74.4°C in different elastomers. The elastomers behave as a good vibration damper both in lower and higher frequency range. Thus these elastomers exhibit good damping behavior in a wide range of temperature and frequency, a primary requirement for practical damping applications. A modal constrained layer damping system constructed utilizing these elastomers exhibits its potentiality to attenuate structural vibrations with respect to mild steel bare plate resonator under laboratory fabricated testing methodology. © 2013 Wiley Periodicals, Inc. *J. Appl. Polym. Sci.* 130: 3611–3623, 2013

KEYWORDS: elastomers; glass transition; properties and characterization

Received 28 January 2013; accepted 1 June 2013; Published online 26 June 2013

DOI: 10.1002/app.39607

INTRODUCTION

Uncontrolled vibrations in structures, dynamic systems, and machines cause fatigue, damage, and structural failure under resonance condition. Therefore, vibration control is a serious engineering challenge. The vibrations and noise control can be reduced by a number of ways. These are generally classified into active and passive methods.^{1–3} The active damping is attained through sensing and activation to suppress the vibration in real time using sensor and actuator which are usually piezoelectric devices.^{4–6} In passive damping, several methods are available. Sometimes, it involves the modification of the system stiffness/mass to alter the resonance frequencies which can reduce the unwanted vibration as long as excitation frequencies remain unchanged. But in most cases, the vibrations need to be isolated or dissipated by using isolator or damping materials.

In passive damping treatments, polymeric materials are extensively used in sound and vibration damping applications because of their inherent damping characteristics.^{7–9} Researchers developed polymeric materials like polymer blend and interpenetrating polymeric network (IPN) as high performance damping materials.^{10,11} The basic principle of the passive damping is the dissipation of vibration energy by transforming it into heat energy. The ability of a material to dissipate vibration energy is defined by loss factor. Loss factor is defined by the

ratio of energy dissipated to energy stored in a cycle of vibration. Dynamic mechanical analysis (DMA) is a very powerful tool for the measurement of damping loss factor of a polymer in a wide temperature and frequency range.¹²

An extensive research work has been already performed on natural oil to obtain functional polymeric materials^{13–18} because of its low production cost, universal availability, and biodegradability.^{19,20} Among the different natural oils, linseed oil is the most abundant, cheap and easily available non-edible oil.²¹ Li and Larock²² synthesized cationic polymeric materials having good damping behavior from soybean oil. Even though, they synthesized cationic polymeric materials from corn and fish oil and characterized by DMA,^{23,24} there are no reported work of DMA characterization in a wide range of frequency and analysis of any damping treatment to attenuate structural vibration using a polymeric material prepared from linseed oil.

In the present study, the damping properties of linseed oil based elastomers have been analyzed through a dynamic mechanical analyzer in a wide range of temperature and frequency. The elastomers are copolymer of linseed oil, styrene (ST) and divinylbenzene (DVB), prepared by cationic polymerization technique. The variation of damping properties of different elastomers has been optimized.

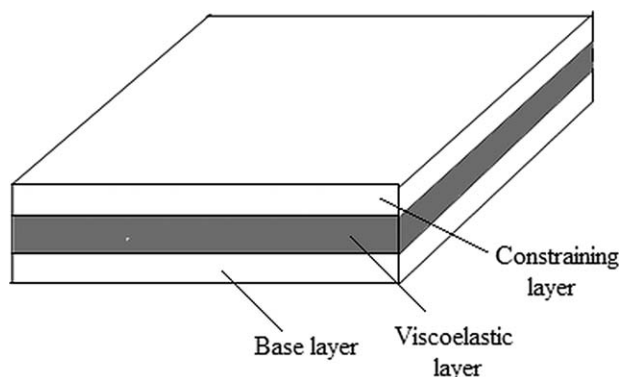


Figure 1. Sketch of a typical CLD system.

The major part of this article is the employment of elastomers for the treatment in constrained layer damping (CLD) to attenuate structural vibration and to study the material performance. The constrained layer or active CLD system uses three layered sandwich system which is formed by laminating base plate to a viscoelastic layer and then adding a constraining layer. In case of CLD, metal or fiber reinforced plastic and for active constraining layer damping, piezoelectric actuator is used as a constraining layer.^{25–27} The constraining layer causes the viscoelastic damping layer to deform in shear, dissipating mechanical energy. A typical constrained layer structure is shown in Figure 1. The CLD configurations provide a highly effective noise and vibration control mechanism in numerous applications like machinery, structural engineering, automobiles, and aircraft applications over a wide range of frequency.^{1,28–30} In our present work, linseed oil based elastomers are used as a viscoelastic damping layer in a modal CLD configuration. A testing system has been fabricated for determining damping loss factor of the test pieces for CLD system. The objective of this fabrication is to provide simpler and cheaper method for investigation of damping behavior of CLD system around room temperature. The frequency response of the CLD system is evaluated in a medium range of frequency (5 Hz to 1.5 kHz) under the cantilevered boundary condition.

EXPERIMENTAL

Materials

Linseed oil used in our study was obtained from the local market of Kolkata. ST, DVB (55 mol % DVB and 45 mol % ethylvinylbenzene) and boron trifluoride diethyl etherate complex were purchased from Sigma-Aldrich, USA. Methanol, dichloromethane, concentrated sulfuric acid were purchased from Merck, India. Potassium hydroxide was purchased from SRL Chemical Co, India.

Preparation of Elastomers from Linseed Oil

The elastomers were synthesized by cationic polymerization technique. Boron trifluoride diethyl etherate was used as initiator and it was modified before its use in polymerization to reduce its reactivity for homogeneous polymerization. The initiator was modified by its mixing with methyl ester of linseed oil in the weight of 3 : 5 with constant stirring at 0°C. Methyl ester of linseed oil was used for better miscibility with initiator,

leading to uniform distribution of initiator in reaction mixtures. Methyl ester was prepared in two consecutive steps in a transesterification process using the methodology of the transesterification double step process.³¹

Polymeric materials were prepared by heating the mixture of concentration of regular linseed oil, ST, and DVB in a glass mold. The desired amount of ST and DVB were added to the linseed oil and the mixture was vigorously stirred. Then, the mixture was cooled and initiator was added slowly with constant stirring at low temperature. After the homogeneous mixing, the resulting mixture was transferred to a glass mold (150 mm × 150 mm × 3 mm) and the mold was then sealed with silicon adhesive. After that, the mold was kept at room temperature for 12 h and then, it was heated sequentially at different temperatures and different time interval such as, at 60°C for 12 h, at 110°C for 24 h, and finally post-cured at 120°C for 3 h. In our experiment, the linseed oil content in the original composition of samples was varied from 45% to 65% and in the remaining aromatic content the ST and DVB are taken in fixed internal ratio of 3 : 2 in SET I and 1 : 1 in SET II. The initiator was maintained at 8% level in all the samples. The detailed feed compositions of different samples are provided in Table I.

Fourier Transform Infrared Spectrometry of Elastomers

The synthesized elastomers are analyzed by attenuated total reflectance (ATR) method of Fourier transform infrared (FTIR) spectrometry. The samples were analyzed by Bruker, Germany FTIR spectrometer (Model: Alpha-E) and the peak was recorded in absorbance. A total of 42 scans at 4 cm⁻¹ resolution were collected to get an average spectrum.

Characterization of Vibration Damping Properties of Elastomers

Vibration damping properties of the elastomers of SET I and SET II on basis of viscoelasticity were determined through dynamic mechanical analyzer. A rectangular specimen of dimension 35 mm × 6 mm × 2 mm was tested in strain controlled tension mode by Metravib Dynamic Mechanical Analyzer (Model: VA 4000) at a fixed frequency of 5 Hz and dynamic strain of 0.0025%. Each specimen was cooled under liquid nitrogen to -50°C and then heated up to 100°C under helium at a heating rate 3 °C/min. The viscoelastic materials usually possess both elastic and viscous properties and the moduli are

Table I. Detailed Feed Compositions of Different Elastomers

SET	Sample ID	Linseed oil (%)	Styrene (%)	Divinylbenzene (%)	Initiator (%)
I	S1Lin45	45	28	19	8
	S2Lin50	50	25	17	8
	S3Lin55	55	22	15	8
	S4Lin60	60	19	13	8
II	S5Lin50	50	21	21	8
	S6Lin55	55	18.5	18.5	8
	S7Lin60	60	16	16	8
	S8Lin65	65	13.5	13.5	8

generally modelled in complex domain. The complex moduli of a typical viscoelastic material are defined by the equation set²;

$$\begin{aligned} E^* &= E' + iE'' = E'(1 + i\eta) \\ G^* &= G' + iG'' = G'(1 + i\eta) \end{aligned} \quad (1)$$

where, E is the elastic modulus in tension/compression and G is the elastic modulus in shear, respectively. The real part of the moduli is associated with its elastic behavior and is defined as storage modulus. The imaginary part of the moduli is associated with its viscous behavior and is defined by loss modulus. The loss factor is defined by η or $\tan \delta$ which is the ratio of loss modulus and storage modulus and measures the material damping capacity. The storage modulus (E'), loss modulus (E''), and damping loss factor ($\tan \delta$) were recorded as a function of temperature. The main relaxation temperature (T_α) of the polymer was obtained from the peak of the loss tangent plot. The cross-link densities (ν_e) were determined from the rubbery modulus plateau based on the theory of rubber elasticity^{8,32};

$$E' = 3\nu_e RT \quad (2)$$

where, E' is the storage modulus (Young's) of the crosslinked polymer in the plateau region, R is the universal gas-constant ($8.314 \text{ J mol}^{-1} \text{ K}^{-1}$), ν_e is the crosslinking density and T is the absolute temperature (K). The variation of loss factor and crosslinking densities was optimized with the varying content of linseed oil of different samples.

As the shear in the viscoelastic core of the CLD system causes the dissipation of excitation energy of different frequencies, the frequency scan of elastomers of SET II were carried out in shear mode on a dynamic mechanical analyzer. The disc samples of $\varnothing 10 \text{ mm} \times 2.5 \text{ mm}$ height were analyzed at 25°C in a fixed dynamic strain 0.001% and in frequency range of 5 Hz to 1 kHz by Metravib Dynamic Mechanical Analyzer (Model: VA 4000). The shear viscoelastic parameters, i.e. the storage modulus (G'), loss modulus (G''), and damping loss factor ($\tan \delta$) were obtained as a function of frequency.

Construction of Specimens for Constrained Layer Damping Treatment

The linseed oil based elastomers were employed to study its performance in constrained layered damping system. A constrained-layer damping system was constructed using a base plate of mild steel as vibrating layer, and an identical plate of mild steel as a constraining layer. The elastomers were sandwiched between vibrating layer and constraining layer. The size of mild steel plate was of $100 \text{ mm} \times 100 \text{ mm} \times 2 \text{ mm}$ whereas the size of elastomer was of $100 \text{ mm} \times 100 \text{ mm} \times 3 \text{ mm}$. The three pieces were fixed together as shown in Figure 1, using a very thin layer of epoxy adhesive. In the experiment, the elastomers having different compositions were used keeping vibrating layer and constraining layer fixed for all systems.

Fabrication of Experimental Set-up and Technique

The bare plate and the sandwiched test piece were tested under cantilevered condition, i.e. the plate is fixed at one edge and other edges were free. The bare plate was tested to validate the measurement system. The base plate was excited by the sinusoidal excitation which was generated by an electrodynamic shaker of MB

Dynamics, USA (Modal 2 Exciter). The shaker was controlled by function generator of Aplab Limited, India (Model FG 2MD) and amplifier of MB dynamics, USA (US-20 W). A sinusoidal waveform of varying frequency and constant amplitude of 500 mV (RMS) was applied with the help of function generator. The response of the bare plate and sandwiched test piece was picked up by piezoelectric accelerometer of Metra Mass-und Frequenztechnik, Germany (Model KS94B.100*/01). The accelerometer was connected with digital storage oscilloscope of Aplab Limited, India (Model D36100C) interfaced with PC, where the resulting wave form is displayed. The schematic of the experimental set up and fixture for holding exciter and test piece are shown in Figure 2. In case of testing of bare plate, the resonance frequencies (f_n) of different mode (n) were noted to determine the magnitude of corresponding mode shape (ϖ) using the plate equation³³;

$$E = \frac{12(1-\nu^2)\rho a^4}{h^2} \times \left(\frac{2\pi f_n}{\varpi} \right)^2 \quad (3)$$

where, E is the Young's modulus of the base material, ρ is the density of the material, ν is the Poisson's ratio of the material, a is the side of the plate, h is the thickness of the plate, f_n is the natural frequency of the n th mode of the plate, and ϖ is the corresponding mode shape function of vibration. A sinusoidal waveform of amplitude 500 mV (RMS) and a varying frequency from 30 Hz to 1.5 kHz was applied to the bare plate in cantilevered condition. The resonance frequencies of different modes were recorded and the corresponding mode shape functions were calculated. The experimental results of mode shape function were compared with theoretical values from the literature.³⁴ The displacement and acceleration waveform of the base plate as a function of frequency are plotted.

The resonance frequencies and half power bandwidth of sandwiched specimens for each mode of vibration from 30 Hz to 1.5 kHz were recorded to calculate loss factor. The loss factor of the bare plate and CLD system was calculated by bandwidth method using the equation³⁵;

$$\eta = 2\zeta = \frac{\Delta f}{f_r} \quad (4)$$

where, η is the loss factor, ζ is the damping ratio, Δf is the half power bandwidth, and f_r is the resonance frequency.

Also, the loss factor is calculated using logarithmic decrement method using the equation³⁵;

$$\eta = 2\zeta = 2 \frac{1}{\sqrt{1 + \left(\frac{2\pi}{\delta}\right)^2}} \quad (5)$$

where, δ is the logarithmic decrement, defined by

$$\delta = \frac{1}{r} \ln \left(\frac{A_i}{A_{i+r}} \right) \quad (6)$$

where, r is the number of cycles, ζ is the damping ratio, A_i is the first significant amplitude, and A_{i+r} is the amplitude after r cycles. This method gives the response of the CLD system under periodic excitation in a lower range of frequency. For experiment using logarithmic decrement method, a sinusoidal waveform of 6 Hz, 10 Hz, and 15 Hz frequency and amplitude of 1.5 V (RMS) was supplied to the shaker. The time decay waveform of the system was recorded by oscilloscope and the loss factor is calculated using this waveform.

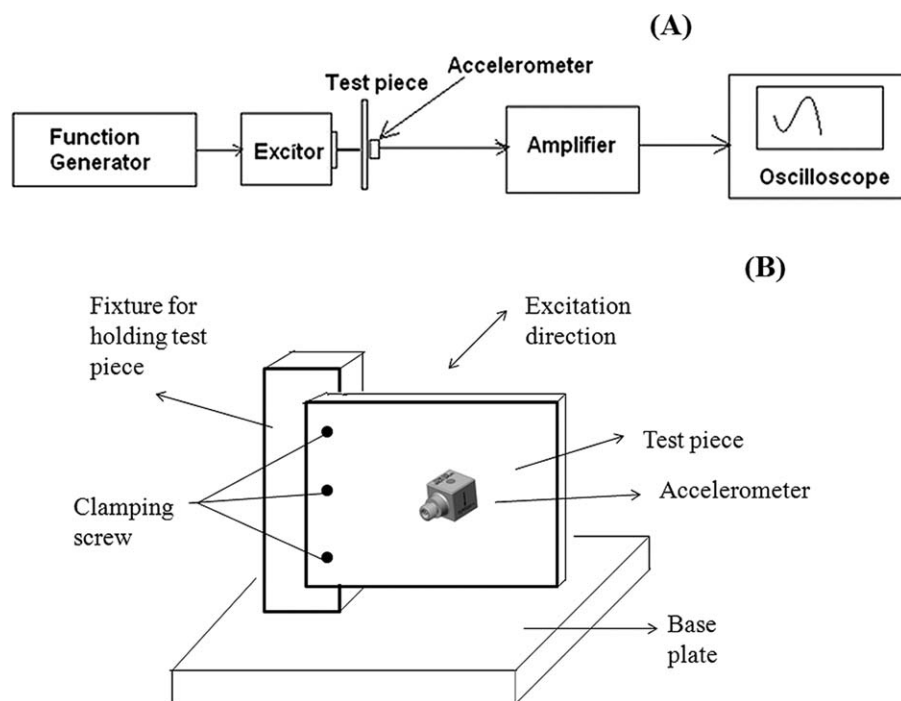


Figure 2. A: Schematic of experimental set up for damping measurement and (B) schematic of fixture for holding exciter and test piece.

RESULTS AND DISCUSSIONS

FTIR Spectroscopy Analysis of the Elastomers

The FTIR spectrum of elastomer (S2Lin50) is shown in Figure 3. The spectrum of sample S2Lin50 is the representative spectrum of all elastomers. The transmittance peak at 1741 cm^{-1} is for the carbonyl group (—C=O) in ester linkage of the oil and it is the characteristic peak of the oil content in the elastomer. The transmittance peak at 690 cm^{-1} is due to —C—H out of

plane bending of aromatic ring of ST and DVB and it is the characteristic peak of aromatic content in elastomer.³⁶ In cationic polymerization reaction, DVB acts as a crosslinker and ST as a comonomer. The main polymer chain is composed of crosslinked polymer of ST and DVB in which the linseed oil molecule is grafted. The schematic of polymerization reaction is shown in Scheme 1. The oil and aromatic part present in elastomers have two part one free part and another crosslinked part.

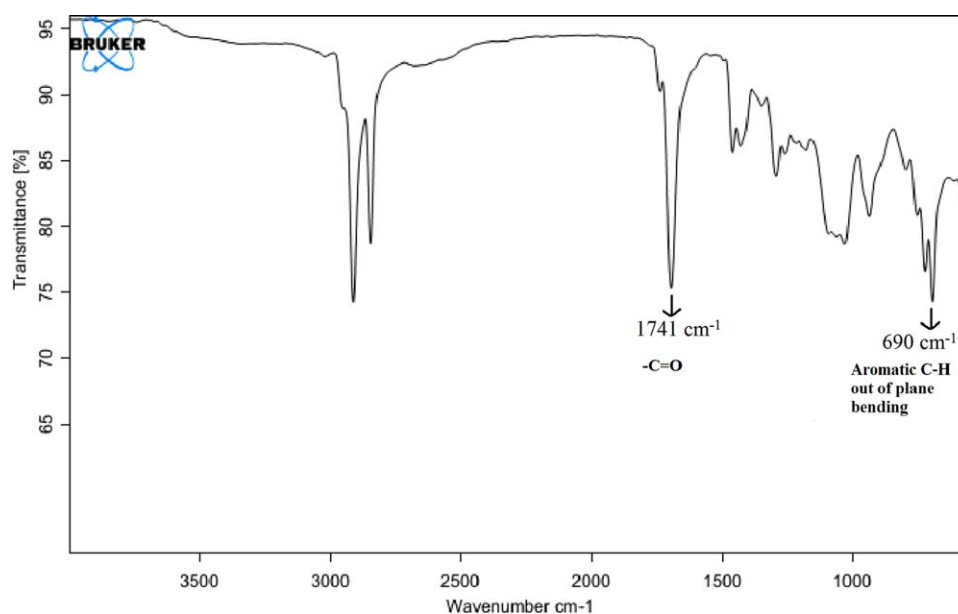
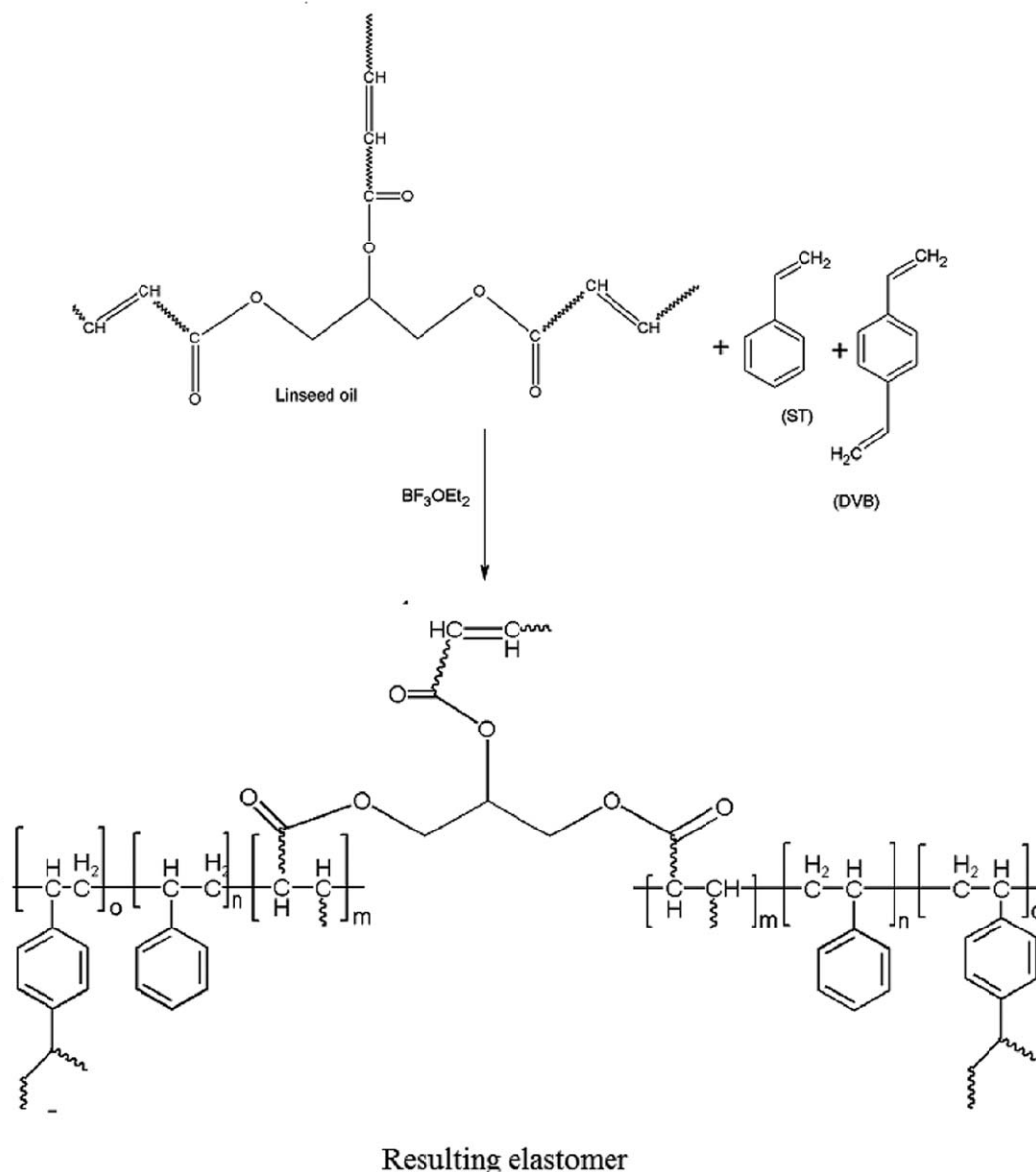


Figure 3. FTIR spectrum of elastomer. [Color figure can be viewed in the online issue, which is available at wileyonlinelibrary.com.]



Scheme 1. Schematic of cationic polymerization reaction.

This free part is viscous and crosslinked part is elastic in nature. Thus, the elastomer is viscoelastic in nature. The free oil as well as other free portion present in elastomers helps in plasticization of the crosslinked insoluble polymers. The crosslinked elastic part has a major effect on the properties of the elastomers.

Damping Properties of the Elastomers

The variations of storage modulus, loss modulus and loss factor with temperature for different elastomers having varying linseed oil concentration are shown in Figure 4. The variation of parameters of SET I in Figure 4 are representatives of DMA of all samples. The main relaxation temperature (T_x), crosslinking densities (ν_e), maximum damping loss factor, $(\tan \delta)_{\max}$ damping loss factor at room temperature, i.e. at 25°C $(\tan \delta)_{rt}$, storage modulus at 0°C (E') and storage modulus at room temperature $(E')_{rt}$ are listed in Table II. In Figure 4, the

temperature dependence of loss factor, storage modulus, and loss modulus are shown in the temperature range of -50°C to 100°C. From Table II, it is clear that damping loss factor improves with an increase in linseed oil concentration in the original compositions of the samples. The T_x shifts to lower temperature with an increase in linseed oil concentration in the original composition of the samples. In $\tan \delta$ vs. temperature curve of Figure 4, a very low intense peak of $\tan \delta$ arises in the temperature range of -50°C to 0°C. The synthesized elastomers have two parts, one crosslinked polymer chain of ST-DVB in which the linseed oil is grafted and second unreacted part comprising free linseed oil and homopolymers of ST and DVB and a small proportion of copolymer of ST-DVB. The grafted linseed oil content and free linseed oil content are determined through spectroscopic characterization technique³⁷ and listed in Table III. The crosslinked part is elastic and unreacted part is

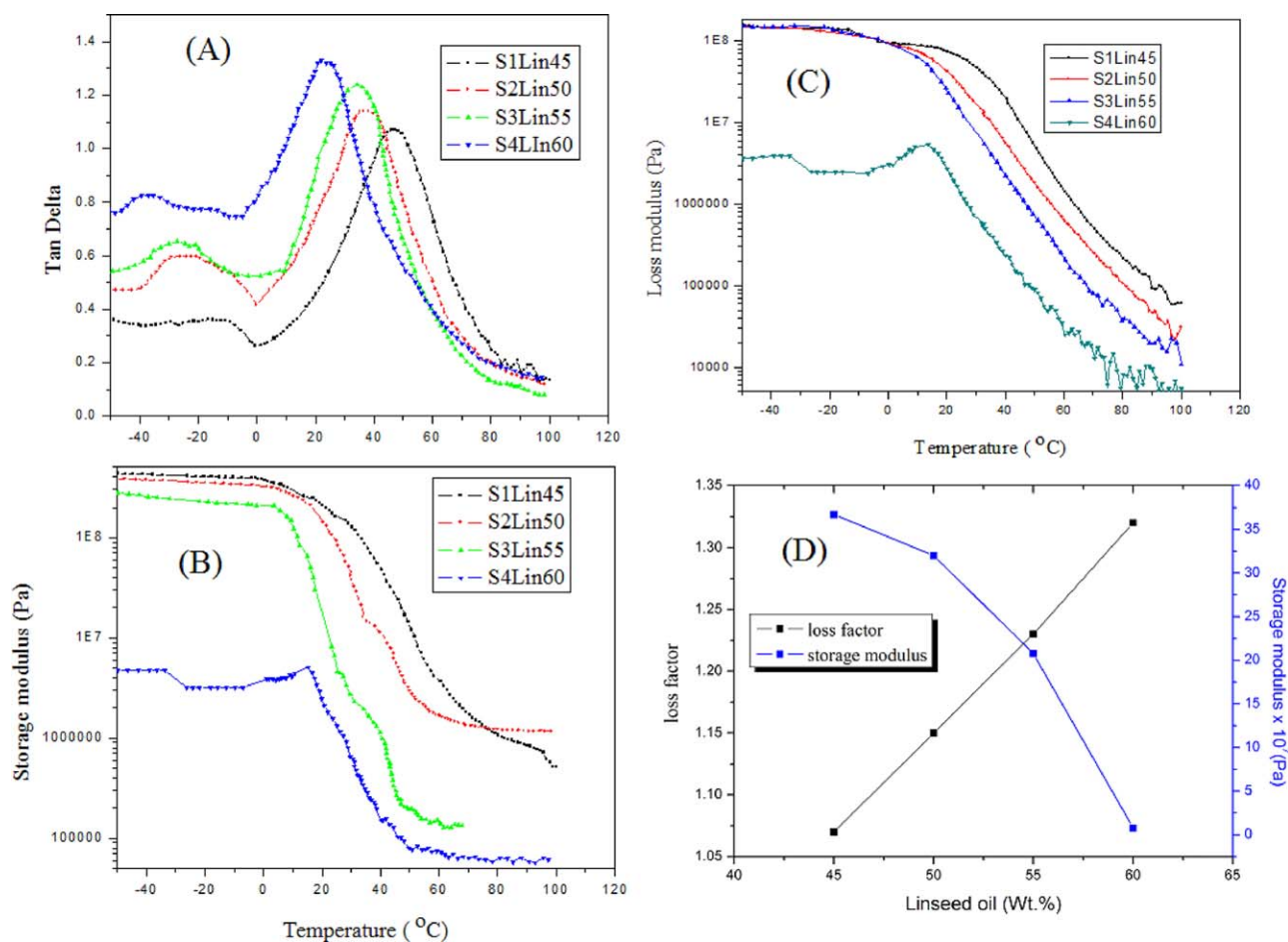


Figure 4. DMA results. A: Variation of $\tan \delta$ with temperature, (B) variation of storage modulus with temperature, (C) variation of loss modulus with temperature, and (D) Variation of loss factor and storage modulus with linseed oil content. [Color figure can be viewed in the online issue, which is available at wileyonlinelibrary.com.]

viscous in nature. The T_x is the relaxation temperature of the crosslinked elastic part. The low intense peak of $\tan \delta$ arises due to presence of free linseed oil which is not thermodynamically miscible with the crosslinked polymer network. Also, there are two segments in the crosslinked polymer chain with different mobility. The linseed oil segment is flexible whereas aromatic ST-DVB segment is rigid. Also, the unreacted linseed oil allows the material to plasticize and soften. The damping, which is energy dissipation, occurs in polymers because of intermolecular friction and molecular relaxation.³⁸ Crosslinking plays an important role in determining the damping behavior of the thermosetting materials.¹² As the degree of crosslinking decreases, the damping property of the polymers improves. The DVB plays as a crosslinker in cationic polymerization as it has two reactive C=C bonds per molecule. Thus, the higher concentration of DVB increases the degree of crosslinking and restricts the motion of the polymer chain which reduces the damping properties. The damping property of elastomers increases with an increase in linseed oil content in the original compositions. Also, the ester group of linseed oil directly attached to the polymer backbone greatly contributes to improve the damping property.³⁹ The increase in linseed oil content means a decrease in DVB

content as a result of which the degree of crosslinking of resulting elastomer decreases. At the same time, the increase in linseed oil content leads to an increase in free oil content in elastomers as described in Table III which has a direct effect to soften crosslinked part of the elastomer. Thus, the increase in linseed oil content in the original compositions of elastomers improves the damping property. The variation of loss factor with linseed oil content in the samples is shown in Figure 4. The loss factor increases linearly with an increase in linseed oil content. The higher DVB content in sample S5Lin50 reduces its damping loss factor with respect to sample S2Lin50 though both have 50% oil in their compositions. The presence of linseed oil in resulting elastomers has a potential effect in resulting elastomers to improve the damping behavior. The samples containing more than 60% oil are not suitable because of low strength. It is required to control the ratio of crosslinked part to viscous part content in resulting elastomers to get optimum damping and proper strength. The loss factor ($\tan \delta$) becomes maximum at primary relaxation temperature (T_x). At primary relaxation temperature or near about it, the chains begin reptate back and forth along their length. The excitation energy dissipates in the crosslinked polymer chain due to this molecular motion which

Table II. Dynamic Mechanical Analysis Result of Elastomers

S E T	Sample ID	Compositions	Dynamic mechanical analysis results								
			T_g (°C)	Crosslinking density $\times 10^2$ (mol/m ³)	$(\tan\delta)_{\max}$	$(\tan\delta)_x$	ΔT (°C)	(E') $\times 10^7$ (Pa)	$(E')_{rt}$ $\times 10^7$ (Pa)	(E'') $\times 10^7$ (Pa)	$(E'')_{rt}$ (Pa)
I	S1Lin45	Oil45+ST28 +19DVB+In8	46.3	4.34	1.07	0.56	72	36.7	16.2	9.38	6.22
	S2Lin50	Oil50+ST25 +17DVB+In8	37.3	3.50	1.15	0.87	70.7	32	9.35	9.03	2.7
	S3Lin55	Oil55+ST22 +15DVB+In8	33	2.53	1.23	1.08	74.4	20.8	0.59	8.3	1.3
	S4Lin60	Oil60+ST19 +13DVB+In8	23.3	1.15	1.32	1.3	69.7	0.76	0.14	0.48	0.12
II	S5Lin50	Oil50+ST21 +21DVB+In8	43.4	4.30	0.79	0.57	63.6	36.5	6.9	9.89	3.87
	S6Lin55	Oil55+ST18.5 +18.5DVB+In8	32.6	2.81	0.78	0.72	69	24.2	2.68	7.45	1.86
	S7Lin60	Oil60+ST16 +16DVB+In8	22.8	2.01	0.87	0.86	67.7	1.00	0.46	0.60	0.34
	S8Lin65	Oil65+ST13.5 +13.5DVB+In8	15.2	1.04	0.95	0.81	50	0.61	0.12	0.33	0.07

transforms excitation energy into heat energy.^{40,41} The glass transition temperature increases with increasing crosslinking density.⁸ As increase in linseed oil content reduces the degree of crosslinking, the T_g shifts to a lower temperature with an increase in linseed oil content in the elastomers.

The high $\tan\delta$ value ($\tan\delta \geq 0.3$) of the materials in a range of broad temperature is very crucial for effective damping.⁴² The temperature ranges (ΔT) for effective damping of elastomers evaluated from plot of $\tan\delta$ versus temperature curve are listed in Table II. The $(\tan\delta)_{\max}$ value of elastomers ranges from 0.78 to 1.32 and ΔT varies from 63 to 74.4°C. In case of sample 8, ΔT is 50°C. In case of samples containing higher concentration of linseed oil (55–65%) in original compositions, the loss factors at lower temperatures (0°C or near 0°C) are always greater than 0.48. The room temperature (25°C) loss factors of the elastomers are in the range of 0.56–1.08 which are much higher than minimum required loss factor for effective damping,⁴² this value is even higher than different polyurethane-based IPN,^{11,39} polymer blend,¹⁰ and comparable to crosslinked composites, hybrids.^{43,44} It is well known that the glass transition region of the polymer exhibits maximum potential for sound and vibration damping.⁷ As the primary relaxation temperature of these elastomers are in the range of 15.2–46.3°C, i.e. around room temperature, they are very appropriate damping materials for practical applications. These elastomers can be employed in different damping configurations which provide highly effective noise and vibration control mechanism in numerous applications.^{1,29}

From the storage modulus plot of Figure 4, it is observed that storage moduli of all samples are high at 0°C and are in the range of 0.608×10^7 to 36.7×10^7 as recorded in Table II. As the temperature increases, the storage moduli exhibit a sharp decrease in the temperature region 10–40°C, which corresponds to a primary relaxation process followed by a rubbery plateau at temperature above 40°C. The sharp drop in storage moduli correspond to the temperature at which $\tan\delta$ is maximum, indicating a maximum dissipation of vibration energy. The storage modulus at 0°C and at room temperature (25°C) increases with an increase in DVB content and decrease in linseed oil content in the original composition of the samples. Storage modulus measures the amount of energy stored in crosslinked structures per

Table III. Grafted and Free Oil Content in Elastomers

SET	Sample ID	Bound oil content (%)	Free oil content (%)
I	S1Lin45	38.4	12.9
	S2Lin50	46.7	13.2
	S3Lin55	43.6	20.5
	S4Lin60	40.1	27.6
II	S5Lin50	45.5	12.5
	S6Lin55	44	19
	S7Lin60	39.5	28.5
	S8Lin65	35	38

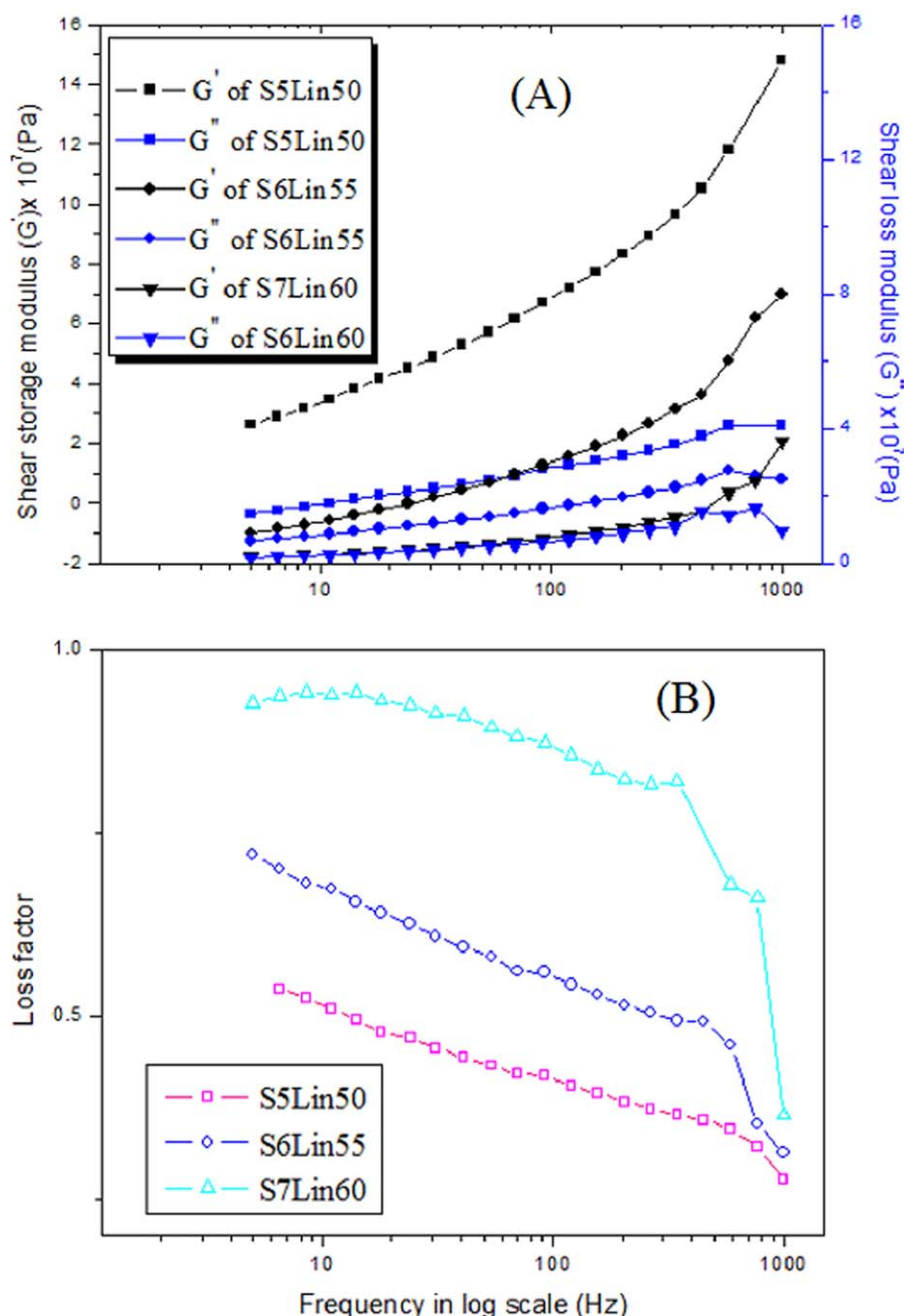


Figure 5. The variation of shear storage modulus, shear loss modulus, and loss factor with frequency. [Color figure can be viewed in the online issue, which is available at wileyonlinelibrary.com.]

cycle of external excitation and it is recoverable strain energy of any specimen under deformation. The highly crosslinked structures absorb more excitation energy than to dissipate as a result of which storage modulus increases. The degree of crosslinking decreases with an increase in linseed oil content and decrease in DVB content. This results in decrease in storage modulus.

In Figure 4, the variation of loss modulus (E'') with temperature is also shown. Like storage moduli, loss moduli of all samples are also high at 0°C and have the range of 9.89×10^7 to 0.33×10^7 Pa as recorded in Table II. It exhibits a sharp decrease in the temperature range of 10°C to 40°C , which

corresponds to $(\tan \delta)_{\max}$ of $\tan \delta$ vs. T curve. The room temperature loss moduli $(E'')_{\text{rt}}$ are in the range of 6.22×10^7 Pa to 0.07×10^7 Pa. Like storage modulus, the loss modulus also decreases with an increase in linseed oil content. In eq. (1), the imaginary part is the loss modulus and it measures the amount of energy dissipated as heat due to deformation of materials. The applied stress which is proportional to applied energy to deform the elastomeric material is higher for highly crosslinked structure. Thus, the loss modulus for highly crosslinked structure is higher as it generates more heat energy due to deformation.

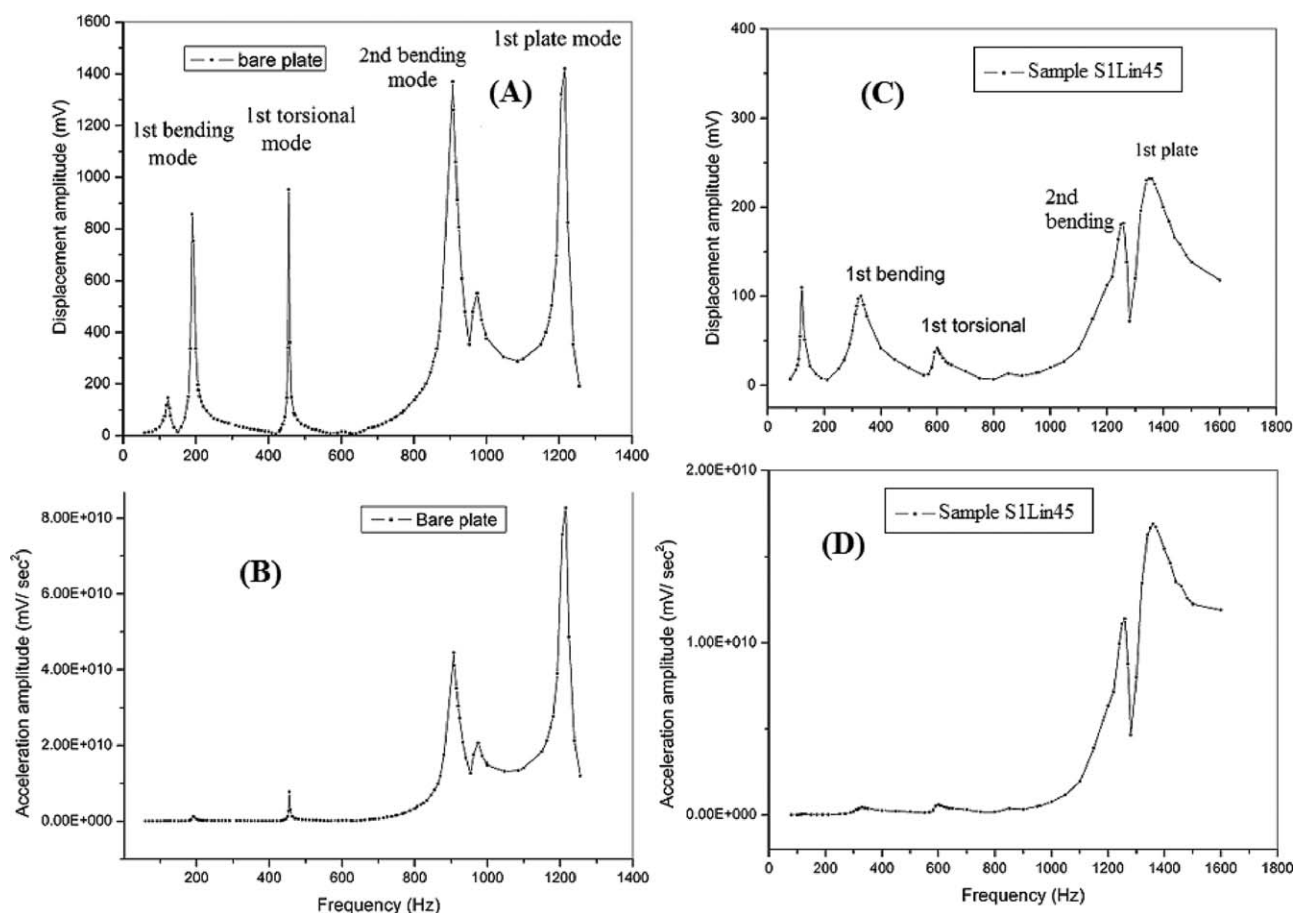


Figure 6. Frequency response of (A) bare plate displacement, (B) bare plate acceleration, (C) CLD system displacement, and (D) CLD system acceleration.

The crosslinking densities as listed in Table II follow the same trend as storage modulus. The elastomer with the highest DVB content (sample S1Lin45) shows highest modulus. There is a decrease in crosslinking density with an increase in linseed oil concentration and decrease in DVB content in the original compositions of the samples. The crosslinking density of the elastomers is proportional to plateau modulus. The plateau modulus increases with an increase of DVB content and decrease in linseed oil content as a result of higher crosslinking density.

The frequency scan of samples of SET II in shear mode was performed in dynamic mechanical analyzer to study viscoelastic properties of the elastomers. The shear storage modulus (G'),

shear loss modulus (G''), and shear damping loss factor ($\tan \delta$) are plotted as a function of frequency in Figure 5. The shear storage modulus and loss modulus increase and the damping loss factor decreases with an increase of frequency. The storage modulus (G') represents the elastic behavior and loss modulus (G'') represents the dissipated energy. Here, the loss factor which is the ratio of G'' to G' predicts about the frequency response of the damping behavior. The frequency response of G' and G'' measures the relative motion of all molecules in the bulk. The increase in elastic modulus G' may result from the change in molecular chain rigidity and the interaction between polymer chains. The increase in G'' arises due to increase in relative motion between polymer chains. The G' increases more

Table IV. Bare Plate Vibration Test Results

Physical parameters of mild steel bare plate	Mode of vibration	Resonance frequency (f_r)(Hz)	Band Width (Δf)(Hz)	Mode shape function (ϖ)value		Loss factor (η)
				Experimental	Theoretical [37]	
$E = 2.1 \times 10^{11} \text{ kg/m}^2$	1 st bending mode	190.4	8	3.82	3.49	0.042
$\rho = 7850 \text{ kg/m}^3$ $\nu = 0.3$	1 st torsional mode	453.8	2.4	9.09	8.54	0.0053
$a = 0.1 \text{ m}$	2 nd bending mode	908	23	18.21	21.44	0.0253
$h = 0.002 \text{ m}$	1 st plate mode	1216	16	24.4	27.46	0.0132

Table V. Loss Factor for CLD Samples Using Bandwidth Method

SET	CLD System using samples	Mode of vibration	Resonance frequency (f_r)(Hz)	Band width (Δf)(Hz)	loss factor (η)	Standard deviation of loss factor (σ)
I	S1Lin45	1 st bending mode	330	54.2	0.164	14×10^{-4}
		1 st torsional mode	602	34.8	0.058	4×10^{-4}
		2 nd bending mode	1260	49	0.039	10×10^{-4}
		1 st plate mode	1355	135	0.1	8.3×10^{-4}
	S2Lin50	1 st bending mode	308	56.7	0.184	15×10^{-4}
		1 st torsional mode	600	37.3	0.062	5×10^{-4}
		2 nd bending mode	1230	94	0.076	3.6×10^{-4}
		1 st plate mode	1353	1.97	0.146	10×10^{-4}
	S3Lin55	1 st bending mode	255.3	54	0.212	13×10^{-4}
		1 st torsional mode	589.8	39	0.066	5.4×10^{-4}
		2 nd bending mode	1152	113	0.098	8.7×10^{-4}
		1 st plate mode	1300	210	0.162	21×10^{-4}
S4Lin60	1 st bending mode	246	55	0.223	15×10^{-4}	
	1 st torsional mode	585	39.8	0.068	6.8×10^{-4}	
II	S5Lin50	2 nd bending mode	1145	123	0.108	10×10^{-4}
		1 st plate mode	1287	220	0.171	14×10^{-4}
		1 st bending mode	360.7	50	0.139	12×10^{-4}
		1 st torsional mode	602	34.7	0.058	7.7×10^{-4}
	S6Lin55	2 nd bending mode	1234	38	0.031	3×10^{-4}
		1 st plate mode	1340	104	0.078	4×10^{-4}
		1 st bending mode	281.7	40.2	0.142	13×10^{-4}
		1 st torsional mode	585	34.3	0.059	5.4×10^{-4}
	S7Lin60	2 nd bending mode	1143	51.9	0.045	3.5×10^{-4}
		1 st plate mode	1291	112	0.087	2.8×10^{-4}
		1 st bending mode	265	44.5	0.168	13×10^{-4}
		1 st torsional mode	582.8	34.45	0.059	3×10^{-4}
	2 nd bending mode	1138	90.6	0.08	1.2×10^{-4}	
	1 st plate mode	1261	141	0.112	6.5×10^{-4}	

steeply than G'' with an increase in frequency, as a result the loss factor slightly decreases with an increase in frequency in case of linseed oil based elastomers. At a fixed temperature, the loss factor of conventional elastomers increases with frequency and exhibits a transition in the higher range of frequency.² But in case of linseed oil based elastomers, there is no transition observed up to 1 kHz applied frequency. The moduli (G' and G'') decrease and loss factor increases with an increase in linseed oil content of elastomers in consistence with previous results. Thus, in Figure 5, the moduli (G' and G'') are lower but $\tan \delta$ is higher in S7 Lin60 than S5Lin50.

Structural Vibration Attenuation Through Constrained Layer Damping Treatment

The bare plate in cantilevered condition was tested to validate the fabricated experimental set up and technique used to evaluate system damping loss factor of CLD system. The bare plate behaves as a resonator under applied vibration and this vibration is controlled through CLD systems. The displacement and

acceleration of bare plate in response to frequency is shown in Figure 6. The natural frequencies of different mode of vibrations, corresponding experimental and theoretical mode shape function values, and loss factors are listed in Table IV. The experimental mode shape function values slightly deviate from theoretical mode shape function values because the boundary condition on plate is not applied in ideal way. The clamping force of the fixed end of the plate and the boundary condition are kept constant throughout the experiment. The frequency response of CLD systems using different elastomers is recorded. The displacement and acceleration of CLD system using sample S1Lin45 as a function of frequency are plotted in Figure 6. It is a representative plot of all systems. The displacement and acceleration amplitude of the CLD system reduces measurably with respect to bare plate. The resonance frequencies of different mode of vibration and corresponding system loss factors for all systems calculated by bandwidth method are listed in Table V. The standard deviation (σ) of each loss factor is also calculated and included in Table V. The variation in system loss factors in

Table VI. Loss Factor of CLD Samples by Logarithmic Decrement Method

Sample	6 Hz		10 Hz		15 Hz	
	loss factor (η)	Standard deviation of loss factor (σ)	loss factor (η)	Standard deviation of loss factor (σ)	loss factor (η)	Standard deviation of loss factor (σ)
Bare	0.0056	4.3×10^{-5}	0.0057	3×10^{-5}	0.0058	4.7×10^{-5}
CLD system using S1Lin45	0.065	4.3×10^{-4}	0.066	5.4×10^{-4}	0.067	5.3×10^{-4}
CLD system using S2Lin50	0.077	4.2×10^{-4}	0.078	2.6×10^{-4}	0.078	3×10^{-4}
CLD system using S3Lin55	0.084	5×10^{-4}	0.085	2.7×10^{-4}	0.087	3.3×10^{-4}
CLD system using S4Lin60	0.093	4×10^{-4}	0.094	3.5×10^{-4}	0.094	3.7×10^{-4}
CLD system using S5Lin50	0.069	2.6×10^{-4}	0.069	3×10^{-4}	0.069	2×10^{-4}
CLD system using S6Lin55	0.073	2.6×10^{-4}	0.075	3×10^{-4}	0.074	2×10^{-4}
CLD system using S7Lin60	0.078	4.5×10^{-4}	0.078	2.5×10^{-4}	0.078	1.3×10^{-4}

various mode are in the range of 0.139–0.223 for 1st bending mode, in the range of 0.078–0.171 for 1st plate mode, in the range of 0.058–0.068 for 1st torsional mode and it varies from 0.031–0.108 for 2nd bending mode. In comparison to base plate loss factor, the loss factor of CLD systems improve 3.3 times to 5.3 times in 1st bending mode, 6 times to 13 times in 1st plate mode, 10 times to 13 times in 1st torsional mode, and 1.2 times to 4.2 times in 2nd bending mode. Thus, the CLD systems exhibit an efficient vibration damping ability. In these CLD systems, the applied external vibration dissipates mainly due to shear in the elastomeric core sandwiched between vibrating base layer and constraining layer. When the base layer undergoes bending vibration, the elastomeric core material is forced to deform in shear, because of the upper stiff base layer. Thus the vibration damping properties of the core materials are very significant. The system loss factor of CLD system increases with an increase in loss factor value of core elastomeric materials. The effect of elastomers comprising varying amount of linseed oil on system damping of CLD systems are optimized. According to DMA, the loss factor of elastomers increases with an increase in linseed oil content. Thus, the loss factor of CLD system increases with an increase in linseed oil content in elastomeric core. The system loss factor increases from CLD system containing sample S1Lin45 to CLD system containing S4Lin60 for SET I and increases from CLD system containing S5Lin50 to S7Lin60 for SET II. In this modal CLD system, the system damping is only observed by varying the core elastomeric materials of finite thickness. The thickness of core materials can also be controlled to get optimum damping. The type of constrained layer materials also affects the damping of CLD system.

The loss factor of bare plate and the loss factor of CLD systems at a lower range of frequency were evaluated by logarithmic

decrement method. The harmfulness caused by low frequency vibration below 10 Hz is very serious such as earth quake, wind induced vibration and track vibration and so on. The elastomers exhibited a good damping behavior in DMA in low frequency range. The time decay curve of bare plate and CLD system comprising sample S1Lin45 is shown in Figure 7. The bare plate waveform exhibits very negligible decay but the CLD system exhibits very sharp decay within 10–15 cycles. The loss factor of bare plate and the system loss factor of CLD systems in 6 Hz, 10 Hz, and 15 Hz applied frequency are listed in Table VI. The standard deviation of loss factor (σ) is also calculated and furnished in Table VI. The loss factor slightly increases with an increase in frequency. The system loss factor increases with

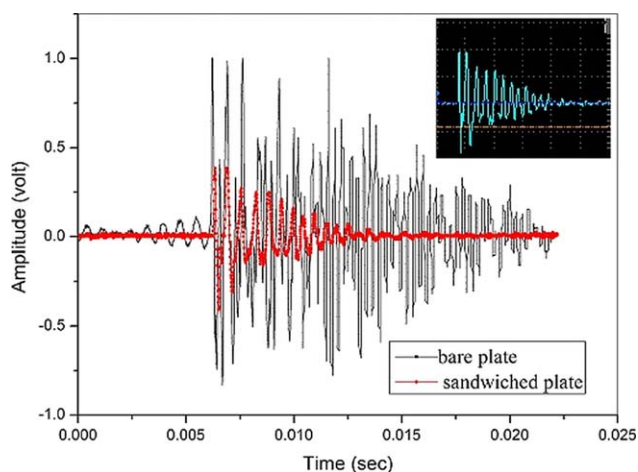


Figure 7. Time decay waveform of bare plate and sandwiched plate using sample S1Lin45 for CLD system. [Color figure can be viewed in the online issue, which is available at wileyonlinelibrary.com.]

variation of elastomers from S1Lin45 to S4Lin60 and S5Lin50 to S7Lin60 for CLD systems in consistent with previous results. In comparison with bare plate loss factor, the system loss factors of different systems increase from 11 times to 16 times at 6 Hz applied frequency. Thus, these CLD systems are also effective to fulfill the requirements of practical damping application.

CONCLUSIONS

A variety of elastomers have been developed from linseed oil having potential applications in vibration damping systems to control unwanted vibrations. The DMA results of the elastomers reveal that the maximum damping loss factor, $(\tan \delta)_{\max}$ varies from 0.78 to 1.32 and temperature range (ΔT) for effective damping ($\tan \delta \geq 0.3$) varies from 63°C to 74.4°C. The room temperature (25°C) loss factor $(\tan \delta)_r$ is in the range of 0.56–1.08. The loss factor increases with an increase in linseed oil content in the elastomer samples. Thus the elastomers exhibit good damping behavior in a wide range of temperature. The damping behavior of elastomers in shear was optimized as a function of frequency at room temperature (25°C) in a frequency range 5 Hz to 1 kHz. The shear storage modulus (G'), shear loss modulus (G'') increases with frequency and the shear loss factor slightly decreases with frequency. The elastomers behave as a good vibration damper both in lower frequency range (around 10 Hz) and higher frequency range (around 1 kHz).

A modal CLD system is constructed employing these elastomers as a core material of sandwiched system. The system loss factors were evaluated in different mode of plate vibration by band width method in the range of 5 Hz to 1.5 kHz. In each mode of vibration the loss factor of the CLD system increases significantly in comparison with the loss factor of the mild steel plate resonator. The loss factor in low frequency range (5–15 Hz) was evaluated by logarithmic decrement method. In comparison with bare plate, the loss factor of different CLD systems is increased from 11 times to 16 times at 6 Hz applied frequency. Thus, this modal CLD systems exhibit an extensive effectiveness to attenuate structural vibration of any frequency from 5 Hz to 1.5 kHz.

ACKNOWLEDGMENT

The financial support under major research project scheme (F.No.36-251(2008) (SR)) from University Grant Commission (UGC), New Delhi, India is highly acknowledged.

REFERENCES

- Nashif, A. D.; Jones, D. I. G.; Henderson, J. P. *Vibration Damping*; Wiley: New York, **1985**.
- Jones, D. I. G. *Handbook of Viscoelastic Vibration Damping*; Wiley Inter science: New York, **2001**.
- Barber, A. *Handbook of Noise and Vibration Control*; Elsevier Science: New York, **2002**.
- Kang, Y. K.; Park, H. C.; Kim, J.; Choi, S.-B. *Mater. Design* **2002**, *23*, 277.
- Raja, S.; Prathap, G.; Sinha, P. K. *Smart. Mater. Struct.* **2002**, *11*, 63.
- Caruso, G.; Galeani, S.; Menini, L. *Simul. Modell. Pract. Theory* **2003**, *11*, 403.
- Sperling, L. H. In *Sound and Vibration Damping with Polymers*; Corsaro, R.D.; Sperling, L.H., Eds., ACS Symposium Series 424; American Chemical Society: Washington, DC, **1990**; p 5.
- Nielson, L. E.; Landel, R. F. *Mechanical Properties of Polymers and Composites*, 2nd ed.; Marcel Dekker: New York, **1994**.
- Klempner, D.; Sperling, L. H.; Utracki, L. A. *Interpenetrating Polymer Networks*, ACS Symposium Series 239; American Chemical Society: Washington, DC, **1994**.
- Yamada, N.; Shoji, S.; Sasaki, H.; Nagatani, A.; Yamaguchi, K.; Kohiya, S.; Azanam, H. S. *J. Appl. Polym. Sci.* **1999**, *71*, 855.
- Qin, C.-L.; Cai, W.-M.; Cai, J.; Tang, D.-Y.; Zhang, J.-S.; Qin, M. *Mater. Chem. Phys.* **2004**, *85*, 402.
- Nielson, L. E. *Mechanical Properties of Polymer and Composites*; Marcel Dekker: New York, **1974**.
- Li, F.; Larock, R. C. *J. Appl. Polym. Sci.* **2001**, *80*, 658.
- Scala, J. L.; Wool, R. P. *Polymer* **2005**, *46*, 61.
- Lu, J.; Wool, R. P. *J. Appl. Polym. Sci.* **2006**, *99*, 2481.
- Khot, S. N.; Lascala, J. J.; Can, E.; Morye, S. S.; Williams, G. I.; Palmese, G. R.; Kusefoglu S. H.; Wool, R. P. *J. Appl. Polym. Sci.* **2001**, *82*, 703.
- Lu, Y.; Larock, R. C. *Biomacromolecules* **2007**, *8*, 3108.
- Lu, Y.; Larock, R. C. *Biomacromolecules* **2008**, *9*, 3332.
- Xia, Y.; Larock, R. C. *Green Chem.* **2010**, *12*, 1893.
- Ronda, J. C.; Lligadas, G.; Galia, M.; Ca'diz, V. *Eur. J. Lipid Sci. Technol.* **2011**, *113*, 46.
- Maccoy, D. Linseed in Favour as a Versatile Crop. *Belfast News Lett.* Apr 26, **2003**.
- Li, F.; Larock, R. C. *Polym. Adv. Technol.* **2002**, *13*, 436.
- Li, F.; Hasjim, F.; Larock, R. C. *J. Appl. Polym. Sci.* **2003**, *90*, 1830.
- Li, F.; Perrenoud, A.; Larock R. C. *Polymer* **2001**, *42*, 10133.
- Capps, R. N.; Beumel, L. L. In *Sound and Vibration Damping with Polymers*; Corsaro, R. D.; Sperling, L. H., Eds., ACS Symposium Series 424; American Chemical Society: Washington, DC, **1990**; p 63.
- Ro, J.; Baz, A. *J. Vib. Control.* **2002**, *8*, 833.
- Shen, I. Y. *ASME J. Vib. Acoust.* **1994**, *116*, 341.
- Rao, M. D. *J. Sound Vib.* **2003**, *262*, 457.
- Nakra, B. C. *J. Sound Vib.* **1998**, *211*, 449.
- Haung, S. C.; Inman, D.; Austin, E. *Smart Mater. Struct.* **1996**, *5*, 301.
- Samios, D.; Pedrotti, F.; Nicolau, A.; Reiznautt Q. B.; Martini, D. D.; Dalcin, F. M. *Fuel. Process. Technol.* **2009**, *90*, 599.
- Flory, P. J. *Principles of Polymer Chemistry*; Cornell University Press: Ithaca, New York, **1953**; chapter 6.

33. Kumar, R.; Shakher, C. In Proceedings of 9th International Symposium on Laser Metrology; Quan, C., Ed.; Singapore, June 30 to July 2, **2008**; SPIE: USA, **2008**.
34. Kumar, R., Shakher, C. *Opt. Lasers Eng.* **2004**, *42*, 585.
35. De Silva, C. W. *Vibration Damping Control and Design*; CRC Press: USA, **2007**.
36. Kumar, G.; Nisha, N. *J. Polym. Res.* **2011**, *18*, 241.
37. Sharma, V.; Banait, J. S.; Kundu, P. P. *Ind. Eng. Chem. Res.* **2008**, *47*, 8566.
38. Chern, Y. C.; Tseng, S. M.; Hsieh, K. H. *J. Appl. Polym. Sci.* **1999**, *74*, 328.
39. Chang, M. C. O.; Thomas, D. A.; Sperling, L. H. *J. Polym. Sci. Part B: Polym. Phys.* **1988**, *26*, 1627.
40. Sperling, L. H. *Introduction to Physical Polymer Science*, 2nd ed.; Wiley Inter science, New York: **1992**.
41. Sperling, L. H.; Fay, J. J. *J. Polym. Adv. Technol.* **1991**, *2*, 49.
42. Trakulsujaritchok, T.; Hourston, D. J. *Eur. Polym. J.* **2006**, *42*, 2968.
43. Xiang, P.; Zaho, X.-Y.; Xiao, D.-L.; Lu, Y.-L.; Zhang, L.-Q. *J. Appl. Polym. Sci.* **2008**, *109*, 106.
44. Xiao, D.; Zhao, X.; Feng, Y.; Xiang, P.; Zhang, L.; Wang, W. *J. Appl. Polym. Sci.* **2010**, *116*, 2143.